

The Impact of Deep Levels on the Photocurrent Transients in Semi-Insulating GaAs

M. PAVLOVIĆ,^{1,2} B. ŠANTIĆ,¹ D.I. DESNICA-FRANKOVIĆ,¹ N. RADIĆ,¹
T. ŠMUC,¹ and U.V. DESNICA¹

1.—Ruder Bošković Institute, Bijenička 54, 10000 Zagreb, Croatia. 2.—E-mail: pavlovic@rudjer.irb.hr

The photocurrent transients, $I_{PC}(t)$, were studied in semi-insulating (SI) GaAs during a low-temperature (low-T) illumination. Unusual transients were explained by the model, relating $I_{PC}(t)$ to the deep levels/traps and their occupancy. Such traps were actually detected and characterized by the independent measurements of the thermally stimulated currents (TSCs). The processes of the generation, recombination, and capture were described by a set of coupled differential equations and solved numerically. The $I_{PC}(t)$, calculated without any free parameter, well reproduced (through eight orders of magnitude) the experimental transients over a wide range of the photon energies and intensities. The best-fit parameters agreed well with those determined from the TSC measurements.

Key words: Photocurrent transients, deep levels/traps, semi-insulating GaAs

INTRODUCTION

The performance of integrated circuits and field effect transistors, based on a semi-insulating (SI), undoped GaAs, is essentially influenced by the quality of the substrate. The quality depends on the concentration of the native defects and unavoidable chemical impurities having deep energy levels in the forbidden energy gap. Besides the well-known EL2 level, there are other deep levels in the undoped, SI GaAs energy gap, which have an impact on the microscopic and macroscopic properties of SI GaAs,^{1–15} including some low-temperature (low-T) transient phenomena.^{4,7–14} It has been shown that the majority of these defects are electron traps.^{1–3} The characterization of the deep traps, which means a determination of their main parameters, and a trap “signature” (particularly activation energy, E_a , and capture cross section, σ) has been the main objective of numerous researches. These results, based on the classical methods of a single-peak analysis, have been analyzed and systematized in Ref. 16. A new approach, which enabled the complete deep-trap characterization (including the trap concentrations),

using a simultaneous multiple-peak analysis method (SIMPA) was recently introduced.^{17,18} Furthermore, after the re-analysis with the SIMPA of the already published thermally stimulated current (TSC) data obtained by over 20 different authors, over a 30-year period, a complete set of all deep traps in the SI GaAs was established.¹⁹

In numerous reports,^{4–10} unusual transients have been observed, which manifest as slow changes in a low-T photocurrent transients ($I_{PC}(t)$) before it finally reaches a constant (saturation) value. In this work, these peculiar $I_{PC}(t)$, measured on the undoped, liquid-encapsulated Czochralski (LEC) SI GaAs, were explained by a model that relates $I_{PC}(t)$ to the deep levels and their occupancy. The presence of such deep levels was proven independently by the TSC measurements. The model assumes that the photo-generated free carriers are trapped into the deep levels, which results in shortening of their free lifetimes, and that the final, stationary value of $I_{PC}(t)$ is reached only after all traps are filled. The processes of the generation, recombination, and capture of charge carriers were described with a pertinent set of coupled differential equations, which were solved numerically, by the procedure in which the Runge–Kutta method was used.²⁰ The photocurrent

(Received December 30, 2002; accepted June 16, 2003)

transients, calculated via the model, very well reproduced the experimentally observed transients over eight orders of magnitude in the $I_{PC}(t)$ changes, as well as over a wide range of intensities and photon energies, E_{ph} , used for the generation of free carriers. The best-fit trap parameters and concentrations agreed well with the ones determined from the TSC measurements. This strongly supports the assumption that the deep levels and their occupancy are directly responsible for peculiar photocurrent transients in a SI GaAs.

The additional byproduct of this analysis was the estimate of the electron and hole mobility in a SI GaAs at low-T, as well as the capture cross sections of the EL2 defect, which all showed good agreement with the previously published results of other authors, obtained by different methods.

EXPERIMENTAL DETAILS

The photocurrent transients at 85 K were measured in the same apparatus used for the TSC measurements described previously.^{3,7} The undoped, LEC SI GaAs samples were used in this study. Each sample was heated in the dark until 340 K (to empty all deep traps/levels) and then cooled in the dark to 85 K. The sample was then illuminated by the photons of the selected wavelength and intensity, and the changes of $I_{PC}(t)$ were recorded until the saturation value was reached. The photon energies lower than the bandgap, E_g , of GaAs were used for photo-excitation because, in that case, the whole sample participates in the absorption, while for $E_{ph} > E_g$ all photons would be absorbed in the very thin surface region. Besides, in such a way, either electrons or holes could be produced preferentially. Namely, for $E_{ph} < E_g$, photogenerated free carriers are created via two processes: the holes are excited to the valence band from the EL2 level and the electrons from the EL2 to the conduction band. The optical cross sections of the EL2 vary considerably with photon energy.²¹ Because of these differences, the 1.2–1.4 eV photons generate preferentially free electrons via the excitations from the EL2 to the conductive band, while for $E_{ph} < 0.8$ eV, the excitation of the holes to the valence band is a preferred process.²¹ A “low” photon intensity (1×10^{13} photons/cm²s) or a “high” intensity (1×10^{15} photons/cm²s) was used in this study. On the same samples, the additional experiment was done, in which the sample was illuminated at 85 K for a prolonged time (1,000 sec), then kept in the dark for the additional 100 sec, followed by a standard $I_{PC}(t)$ measurement.

RESULTS AND DISCUSSION

Photocurrent Transients in Semi-Insulating GaAs

A photocurrent is generally proportional to $(\Delta n \mu_n + \Delta p \mu_p)$ ²² where Δn , Δp , μ_n , and μ_p represent the excess concentrations and mobilities of the electrons and holes, respectively, generated by a light, in respect to the dark values. These values depend on

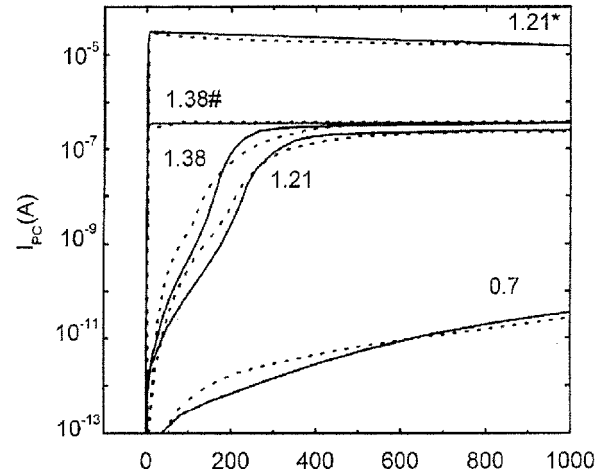


Fig. 1. The measured (dotted curves) and the calculated photocurrent transients (solid curves) for the photon energies 0.7 eV, 1.21 eV, and 1.38 eV with the photon flux of 1×10^{13} photons/cm²s. The curves 1.21* refer to the photon flux of 1×10^{15} photons/cm²s. The curves denoted as 1.38# present the measured (dotted) and the calculated (solid) photocurrents with all deep traps initially full (no transient observed).

factors, such as light intensity, absorption coefficient, photon energy, etc. It has been noticed that the photocurrent exhibits various temporal dependencies during the illumination.^{7,9,10,23–25} The dotted curves on Fig. 1 show the measured photocurrent transients at 85 K. The transients 1.21 eV and 1.38 eV are characterized with the distinguishable gradual increase of the photocurrent occurring in several stages. In both cases, the saturation values were reached after few hundred seconds. For these E_{ph} and the low light intensity, the total rise of the photocurrent during the transient measurement spanned over six orders of magnitude. For the low intensity excitation, all stages of the transient were slow enough to be clearly visible on the time scale of hundreds of seconds.

When the sample was illuminated with high intensity light, an abrupt increase in the photocurrent for more than eight orders of magnitude occurs (Fig. 1, dotted curve 1.21* eV). In this case, all characteristic phases of the transient became very short because of the much faster generation of the free carriers. However, for this strong light intensity, the quenching of the photocurrent can be noticed, starting immediately after the initial abrupt rise of I_{PC} . This is caused by the transition of the EL2 level to the metastable state, EL2*. This process is observable only at high light intensities and for certain photon energies.^{26,27} In an additional experiment, where the $I_{PC}(t)$ was measured after a long pre-illumination at a low-T, no transient was observed. Namely, the I_{PC} saturation value was reached a few seconds after the light was turned on.

Model

To explain qualitatively and quantitatively the characteristic features of the previously described transients, a theoretical model was created and applied to the SI GaAs material. The model assumes

that the deep levels and their occupancy are responsible for the observed photocurrent transients. It was supposed that at the beginning of the illumination, when all deep traps are empty, the capture processes into the deep traps dominates over recombination. This made the effective free-carriers' lifetimes shorter than in the stationary state. The trap with the biggest capture cross section was assumed to fill first, determining the lowest stage of the $I_{PC}(t)$. Subsequently, the traps with the smaller capture cross sections also become filled, which results in the gradual increase of the average free-carrier lifetime and, hence, the increase of the I_{PC} . The photocurrent reaches a constant value when all traps are filled, and traps cease to influence the lifetime and I_{PC} . The stationary lifetime and the stationary, $I_{PC}(\infty)$, then become determined by the main recombination center, by the balance of the processes of the generation and recombination of the photogenerated carriers, respectively. Figure 2 presents the relevant deep levels, assumed trapping, and the recombination scheme included into the model.

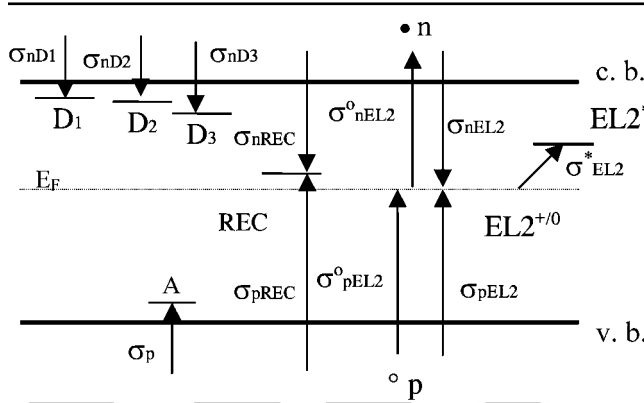


Fig. 2. The model of the SI GaAs bandgap with all the levels and processes (with respective cross sections) included. The term D_i , $i = 1, 2, 3$, denote electron traps, a hole trap, and REC recombination center. The Fermi level (E_F) is pinned to the EL2, situated in the middle of the forbidden energy gap. The terms v. b. and c. b. are the valence and conductive band, respectively. EL2* presents the metastable state of the EL2 defect.

- The EL2 level, an omnipresent and well-known defect in the undoped SI GaAs crystals, is generally found in concentrations of approximately $2 \times 10^{16} \text{ cm}^{-3}$.²⁸ (In the samples used in this work, the presence and the concentration of the EL2 defect was determined by the optical absorption measurements.²⁹) This level plays a triple role here. The first one is a creation of the free electrons and holes in the excitation processes characterized by the optical cross sections ($\sigma_{nEL2}^0(\lambda)$ and $\sigma_{pEL2}^0(l)$, respectively²¹). The second one is the recombination characterized by the capture cross sections for electrons (σ_{nEL2}) and holes (σ_{pEL2}). The calculated values for the capture cross sections (σ_{nEL2} and σ_{pEL2}) are presented in Table I. Finally, the third one addresses the transition, $EL2 \rightarrow EL2^*$, characterized by the cross section $\sigma_{EL2}^*(\lambda)$.
- Three donors (electron traps), D_1 (σ_{nD1}), D_2 (σ_{nD2}), and D_3 (σ_{nD3}), were used in our model. Namely, 11 different deep traps (levels) were determined independently in these SI GaAs samples by the TSC measurements,^{3,17–19} most of them being electron traps. The complete signatures of these traps can be found in Table II (including

Table I. The Characteristic Trap Parameters of the Levels Included in the Model*

Level	N_i/cm^{-3}	σ_{ni}/cm^2	σ_{pi}/cm^2
D_1	1.5×10^{15}	2.0×10^{-16}	—
D_2	2.0×10^{15}	6.0×10^{-17}	—
D_3	8.8×10^{14}	8.0×10^{-18}	—
A	1.0×10^{14}	—	8.0×10^{-17}
REC	1.5×10^{15}	1.8×10^{-18}	4.0×10^{-17}
EL2	2.0×10^{16}	2.5×10^{-19}	3.5×10^{-21}

* The term N_i is the trap concentration, and σ_{ni} and σ_{pi} are the capture cross sections for the electrons and holes, respectively, determined as the best-fit parameters from the fit of the Eq. 11 to the experimental $I_{PC}(t)$ for all used photon energies and light intensities. The starting values of σ_{ni} and σ_{pi} were taken from Refs. 17–19 (Table II). The concentration of the EL2 level was determined from the absorption measurement.²⁹

Table II. The Deep Trap Parameters Obtained by the Simultaneous Multiple-Peak Analysis Method of the Thermally Stimulated Current Spectra (Refs. 17–19) Measured at the Undoped Semi-Insulating GaAs Samples Also Used in the I_{PC} Measurements of This Work

Trap	$E_{a,i}/\text{eV}$	σ_i/cm^2	N_i/cm^{-3}
T_0	0.152 ± 0.004	$(3.2 \pm 0.3) \times 10^{-17}$	$2.4 \times 10^{11} < N_{T0} < 3.0 \times 10^{13}$
T_1	0.158 ± 0.004	$(2.5 \pm 0.4) \times 10^{-18}$	$4.1 \times 10^{12} < N_{T1} < 4.0 \times 10^{14}$
T_{2a}	0.202 ± 0.004	$(2.7 \pm 0.4) \times 10^{-17}$	$2.2 \times 10^{13} < N_{T2a} < 4.0 \times 10^{14}$
T_{2b}	0.229 ± 0.006	$(2.8 \pm 0.8) \times 10^{-17}$	$1.8 \times 10^{12} < N_{T2b} < 3.0 \times 10^{15}$
T_3	0.271 ± 0.004	$(4.9 \pm 0.5) \times 10^{-17}$	$4.1 \times 10^{12} < N_{T3} < 2.0 \times 10^{16}$
T_4	0.281 ± 0.005	$(1.2 \pm 0.6) \times 10^{-17}$	$3.7 \times 10^{12} < N_{T4} < 1.0 \times 10^{15}$
T_{4a}	0.325 ± 0.008	$(1.0 \pm 0.2) \times 10^{-17}$	$3.1 \times 10^{13} < N_{T4a} < 3.0 \times 10^{14}$
T_5	0.439 ± 0.006	$(0.9 \pm 0.1) \times 10^{-15}$	$2.4 \times 10^{14} < N_{T5} < 5.0 \times 10^{15}$
T_6	0.478 ± 0.007	$(3.8 \pm 0.8) \times 10^{-16}$	$3.5 \times 10^{15} < N_{T6} < 5.0 \times 10^{16}$
T_7	0.519 ± 0.006	$(1.1 \pm 0.4) \times 10^{-16}$	$4.8 \times 10^{15} < N_{T7} < 1.0 \times 10^{16}$
T_8	0.578 ± 0.004	$(5.0 \pm 1.5) \times 10^{-16}$	$5.0 \times 10^{13} < N_{T8} < 3.0 \times 10^{15}$
EL2	0.75 ± 0.02	—	—

their concentration ranges). Their concentrations were taken here as fitting variables. Picking up the three characteristic electron traps from the preceding set of 11, representing a fast, medium, and slow trapping, respectively, is deemed as a sensible compromise; including just one electron trap clearly introduced in the simulation a two-step transient of the $I_{PC}(t)$ (not shown), resulting in a poor fit of the experimental curve. On the other hand, the inclusion of more and more traps resulted, understandably, in a progressively better accordance of the measured and simulated $I_{PC}(t)$, but also made the formulas/calculations more cumbersome and, consequently, the basic idea of the model less transparent. Furthermore, the use of just three representative levels (fast, medium, and slow trapping) makes this model more universal and easily applicable for use in the analogous analysis of other GaAs samples and other SI III-V semiconductors or alloys in which similar transients were observed.^{4–10} The best-fit parameters of these three deep-electron traps are presented in Table I.

- One acceptor (a hole trap), denoted as A (σ_{pA}), representing the hole traps, is also included into the model. Namely, (at least one) hole trap was found in these samples,³ and besides, it is known that the hole traps often exist in the SI GaAs material.³⁰ The relevant best-fit capture cross section for the holes (σ_{pA}) and the concentration (N_A) are also presented in Table I.
- The next assumption of the model is that, beside the recombination through the EL2 level, there exists another recombination center (denoted as REC), characterized by the capture cross sections for the electrons (σ_{nREC}) and holes (σ_{pREC}). All data referring to REC (Table I) emerged from the analysis of the model, but it is well-known that such centers unavoidably exist in the SI GaAs.^{1,2}

The simulation starts with the selection of the initial values of all computed functions corresponding to the actual experimental situation. After cooling to a low-T (85 K) in the dark, all deep traps are empty, and the Fermi level (E_F) is situated at the EL2 level in the middle of the gap. When the sample is illuminated with photon energy smaller than the bandgap ($E_{ph} < E_g$), various transitions between bands and localized levels are possible. However, the optically induced trap-to-trap transitions could be neglected because they have a low probability caused by the small product of their concentrations and relatively large average spatial distance among them. It is also assumed that the thermal emission from the deep traps can be neglected because of the fact that in the SI GaAs practically all of these traps release charge carriers at temperatures higher than 90 K ($T > 90$ K), as determined from the TSC measurements.^{1–3,15} The additional plausible assumption is that the EL2 is the only optically active level, i.e., that the processes of the optically stimulated

capture and emission for the other deep levels can be neglected. Furthermore, a direct recombination is also a process with a low probability as well as a direct generation of the free carriers because the photon energies used in this work were smaller than the bandgap of the SI GaAs. Hence, both of these processes were disregarded.

The model proposed leads to a set of coupled differential equations. The first equation presents the time dependence of the free electron concentration, n :

$$\frac{dn}{dt} = \Phi \sigma_{nEL2}^o n_{EL2} - v_n n \times \left[(N_{D1} - n_{D1}) \sigma_{nD1} + (N_{D2} - n_{D2}) \sigma_{nD2} + (N_{D3} - n_{D3}) \sigma_{nD3} + (N_{REC} - n_{REC}) \sigma_{nREC} + (N_{EL2} - n_{EL2}) \sigma_{nEL2} \right] \quad (1)$$

The terms N_{EL2} and N_{REC} are the total concentrations of the EL2 and REC levels, respectively. The term N_{Di} , with $i = 1, 2, 3$, is the total concentration of the relevant electron traps, while n_{Di} is the concentrations of the electrons in them. Similarly, the electron concentration in the REC is denoted as n_{REC} . The first term on the right side of Eq. 1 describes the generation of the free electrons from the EL2 level and is proportional to the light intensity, Φ (in photons/cm²s); the optical cross section for the emission of the electrons from the EL2 level, σ_{nEL2}^o ; and the concentration of the occupied EL2, n_{EL2} . The second term is composed of five similar terms, all of which cause a decrease in n . The term v_n is the thermal velocity for the electrons, $v_n = \sqrt{8kT/\pi m_e^*}$, with $m_e^* = 0.067 m_0$, where m_e^* is the effective electron mass, and m_0 is the electron mass at rest, while k denotes the Boltzmann constant. The first three products describe a capture of the free electrons to different electron traps, while the other two describe a capture of the free electrons into the REC and EL2 levels.

A similar equation describes the change of the concentration of the free holes with illumination:

$$\frac{dp}{dt} = \Phi \sigma_{pEL2}^o (N_{EL2} - n_{EL2}) - v_p p \times \left[n_{REC} \sigma_{pREC} + n_{EL2} \sigma_{pEL2} + (N_A - n_A) \sigma_{pA} \right] \quad (2)$$

All terms in Eq. 2 are of the same structure as the terms in Eq. 1 with analogous meanings of the symbols. The first term on the right side of the Eq. 2 describes the emission of the free holes from the EL2 center to the valence band, while the other three terms describe a capture of the holes into the REC, EL2, and a hole trap A, respectively. The v_p denotes the hole thermal velocity, $v_p = \sqrt{8kT/\pi m_p^*}$, with $m_p^* = 0.45 m_0$, where m_p^* is the effective hole mass. The temporal changes of the populations in the electron (hole) traps included in our model are described by the Eqs. 3–6:

$$\frac{dn_{Di}}{dt} = v_n \sigma_{nDi} (N_{Di} - n_{Di}) n \quad (3-5)$$

where $i = 1, 2, 3$.

$$\frac{dp_A}{dt} = v_p \sigma_{pA} (N_A - p_A) p \quad (6)$$

Equations 7 and 8 show the time dependence of the electron populations in the REC and EL2 centers, respectively:

$$\frac{dn_{\text{REC}}}{dt} = v_n \sigma_{n\text{REC}} (N_{\text{REC}} - n_{\text{REC}}) n - v_p \sigma_{p\text{REC}} n_{\text{REC}} p \quad (7)$$

$$\begin{aligned} \frac{dn_{\text{EL2}}}{dt} = & v_n \sigma_{n\text{EL2}} (N_{\text{EL2}} - n_{\text{EL2}}) n - v_p \sigma_{p\text{EL2}} n_{\text{EL2}} p \\ & - \Phi (\sigma_{n\text{EL2}}^0 + \sigma_{\text{EL2}}^*) n_{\text{EL2}} + \Phi \sigma_{p\text{EL2}}^0 (N_{\text{EL2}} - n_{\text{EL2}}) \end{aligned} \quad (8)$$

The first right side term in Eq. 7 (Eq. 8) describes a capture of the free electrons into the REC center (EL2), while the second term represents a capture of the free holes into them. The third and fourth terms in Eq. 8 represent the optical emission of the electrons from the EL2 into the conduction band and the emission of the holes from the EL2 to the valence band. In fact, n_{EL2} slightly depends on the EL2 \rightarrow EL2* transition, characterized by the cross section σ_{EL2}^* . This dependence is included in the third right-hand term of Eq. 8 as well as by Eq. 9, which describes temporal change of the EL2* concentration, n_{EL2^*} :

$$\frac{dn_{\text{EL2}^*}}{dt} = \sigma_{\text{EL2}}^* \Phi n_{\text{EL2}} \quad (9)$$

However, this influence is negligible up to very high light intensities because σ_{EL2}^* is very small in the whole range of the applied E_{ph} (10^{-21} – 10^{-17} cm²).²⁶

Equation 10 presents the condition for charge neutrality:

$$\begin{aligned} n + N_A + n_{\text{EL2}} + n_{\text{EL2}^*} + n_{\text{REC}} + n_{\text{D}_1} + n_{\text{D}_2} + n_{\text{D}_3} \\ = p + p_A + N_{\text{EL2}} + N_{\text{REC}} + N_{\text{D}_1} + N_{\text{D}_2} + N_{\text{D}_3} \end{aligned} \quad (10)$$

Finally, $I_{\text{PC}}(t)$ can be calculated as

$$I_{\text{PC}}(t) = K(bn(t) + p(t)) \quad (11)$$

where the proportionality constant K is defined as a product of the electron charge (e), the electric field at the sample (E), the hole mobility (μ_p), and the area of the contacts (A): $K = eE\mu_p A$, while b denotes the mobility ratio defined as $b = \mu_n/\mu_p$. In the calculations we took, $b = 10$, according to the values estimated in the Refs. 12 and 31. The previously introduced set of coupled differential equations is not analytically solvable. Hence, it had to be solved numerically.

Photocurrent Transient Simulations

To integrate the differential Eqs. 1–9, a computer program was developed based on the Runge–Kutta method²⁰ with a variable step size. The assumptions of the model define the initial conditions. The initial values of both free electron and free hole concentrations before illumination are negligible. An important parameter in the calculations is the initial occupancy of the EL2 level, i.e., the fraction, $f_i = n_{\text{EL2}}/N_{\text{EL2}}$. A convergence of the theoretical curve (photocurrent simulation) is greatly influenced by this parameter:

the small f_i (EL2 level practically empty) favors the hole transitions from the valence band to the EL2, while large f_i (EL2 almost full) prefers the electron transitions from the EL2 to the conduction band. From the independent absorption measurements and analysis on the same samples we have obtained:³² $0.8 \leq f_i \leq 1$. Hence, the values of f_i from that range were used as the initial f_i in our simulations. The best fits were always obtained with $f_i = 0.9$.

Full lines in Fig. 1 show the best fit of Eq. 11 to the experimental $I_{\text{PC}}(t)$ (dotted curves) for the photon energies of 0.7 eV, 1.21 eV, and 1.38 eV (a low light intensity) and 1.21* eV (* denotes a high light intensity regime). The same trap parameters (within 5%) were obtained for all used photon energies in both light intensity regimes. Note that there were no additional free, adjustable parameters, despite a wide range of photon energies and light intensities. The 1.38# curves represent calculated (solid) and measured (dotted) photocurrents in the case when all deep traps are full (in this experiment the sample was initially pre-illuminated at 85 K, which is in simulations equivalent to the initial values for $n_{\text{D}_i}/N_{\text{D}_i}$ and p_A/N_A selected as 1). The comparison of the calculated $I_{\text{PC}}(t)$ with the experimental ones shows a very good qualitative and a good quantitative agreement as well. Most of the characteristic features of the experimental curves were successfully reproduced in the simulated transients for all respective photon energies and light intensities. This includes a gradual increase in I_{PC} and almost the same temporal development over the full range of eight orders of magnitude. Furthermore, the calculated final I_{PC} values after a long (1,000 sec) illumination, which spans over six orders of magnitude depending on the illumination conditions, excellently agree with the experimental values. Finally, in both experimental and calculated curves for the full deep-level regime (1.38# curves in Fig. 1), an abrupt increase in the final I_{PC} was obtained (without gradual changes), giving additional proof that the characteristic transients are caused by the deep levels and their occupancy.

High intensity, 1.21* eV curves were also very similar, both characterized by an abrupt jump of I_{PC} at the beginning of the illumination followed by a slight decrease of I_{PC} with time afterwards. A slow decrease originates from the transition of the EL2 to the metastable state, which is observable only at high light intensities.^{26,27} The best fit gave the optical cross section for the preceding transition, $\sigma_{\text{EL2}}^* = 1 \times 10^{-18}$ cm², which is in a good agreement with $\sigma_{\text{EL2}}^* = 1.23 \times 10^{-18}$ cm², calculated in Ref. 26 from the analysis of the photocapacitance transient measurement at $E_{\text{ph}} = 1.15$ eV.

Table I presents the best-fit parameters for all six levels used in the simulations. The obtained values for the capture cross sections and the trap concentrations are in accordance with the values for the deep levels determined from the independent measurements via the TSC^{17,18} performed on the same

set of the SI GaAs samples. All trap parameters, presented in Table II, also agree well with the values obtained from the re-analysis of a large number of the SI GaAs samples with other methods by different authors, reviewed in Ref. 19.

For the main deep-donor EL2, the capture cross sections for both electrons and holes were calculated from the simulations as well. The obtained result for $\sigma_{n,EL2} = 2.5 \times 10^{-19} \text{ cm}^2$ is 2.9 times smaller than the one calculated according to the formulae $\sigma_n = 6 \times 10^{-15} \exp(-0.066/kT) \text{ cm}^2$, supposedly valid for the temperature range from 50–275 K,³³ which is $7.2 \times 10^{-19} \text{ cm}^2$. However, exactly the same discrepancy was obtained by Look and Fang.³⁴ Furthermore, Look and Fang calculated the capture cross section ratio $\sigma_{n,EL2}/\sigma_{p,EL2}$ to be 70. From our results in this work, that ratio is 71.4, which is again in a very good agreement.

The calculated deep-trap filling dynamics in a low intensity regime and the applied photon energies (not shown) confirmed that all traps get fully filled in the first 200–300 sec, i.e., just in the time interval in which the characteristic features of the transients in $I_{PC}(t)$ were observed (Fig. 1).

Table III shows the best-fit results for the free electron (hole) saturation values, $n(\infty)$ ($p(\infty)$) for each photon energy used. For each photon energy, the constant K in Eq. 11 was calculated from the expression: $K = I_{PC}(\infty)/(10n(\infty) + p(\infty))$, where $I_{PC}(\infty)$ is a measured saturation photocurrent value. The hole mobility (at 85 K) can then be calculated from $\mu_p = K/(eEA)$, yielding $\mu_p = 0.75 \times 10^4 \text{ cm}^2/\text{Vs}$. Assuming $\mu_n = 10 \mu_p$, one gets $\mu_n = 0.75 \times 10^5 \text{ cm}^2/\text{Vs}$. This result is reasonably close to $\mu_n = 1 \times 10^5 \text{ cm}^2/\text{Vs}$, calculated by Look for a SI GaAs when all scattering mechanisms in the SI GaAs were taken into account.³⁵

CONCLUSIONS

Low-T photocurrent transients measured on undoped, SI LEC GaAs samples, illuminated with photon energies smaller than the forbidden energy gap, were simulated by a theoretical model, which connects a temporal development of the photocurrent with the actual deep levels (found in that material) and their occupancy. The model quantitatively reproduced and observed the experimental transients and their changes over eight orders of magnitude

during the illumination, as well as the dependence on the photon energy and the light intensity. Used trap signatures as well as the calculated defect concentrations obtained from simulations of $I_{PC}(t)$ agree well with those obtained by an independent quantitative analysis of the TSC spectra. Furthermore, the presented analysis enabled verification of the cross sections for the electrons and holes of the EL2 defect, the cross section for the transition into metastable state EL2*, as well as the calculation of the electron and hole mobilities in the SI GaAs at 85 K. The obtained values agree very well with the previously reported values of these parameters obtained by other authors via different experimental and theoretical methods.

All these results give strong evidence that those deep levels/traps and the changes in their occupancy during a low-T illumination are directly responsible for the characteristic photocurrent transients observed in the SI GaAs.

REFERENCES

1. A.L. Lin and R.H. Bube, *J. Appl. Phys.* 47, 1859 (1976).
2. A.L. Lin, E. Omelianovski, and R.H. Bube, *J. Appl. Phys.* 47, 1852 (1976).
3. B. Šantić and U.V. Desnica, *Appl. Phys. Lett.* 56, 2636 (1990).
4. W.C. Mitchell and J. Jimenez, *J. Appl. Phys.* 75, 3060 (1994).
5. U.V. Desnica and B. Šantić, *J. Appl. Phys.* 67, 1408 (1990).
6. J. Jimenez, P. Hernandez, J.A. de Saja, and J. Bonnafe, *Phys. Rev. B* 35, 3832 (1987).
7. U.V. Desnica and B. Šantić, *Appl. Phys. Lett.* 54, 810 (1989).
8. U.V. Desnica, D.I. Desnica, and B. Šantić, *Appl. Phys. Lett.* 58, 278 (1991).
9. J. Jimenez, M.A. Gonzales, P. Hernandez, and J.A. de Saja, *J. Appl. Phys.* 57, 1152 (1985).
10. J. Jimenez, P. Hernandez, and J.A. de Saja, *Solid State Commun.* 55, 459 (1985).
11. H.J. Queisser, *Annalen der Physik* 47, 461 (1990).
12. U.V. Desnica, D.I. Desnica, and B. Šantić, *J. Phys.: Condens. Matter* 3, 5817 (1991).
13. T. Benchigner, B. Mari, C. Schwab, and U.V. Desnica, *Jpn. J. Appl. Phys.* 31, 2669 (1992).
14. M. Beaumler, U. Kaufmann, and J. Windscheif, *Appl. Phys. Lett.* 46, 781 (1985).
15. Z.-Q. Fang and D. Look, *Mater. Sci. Forum* 83–87, 991 (1992).
16. D.I. Desnica, *J. Electron. Mater.* 21, 463 (1992).
17. M. Pavlović and U.V. Desnica, *J. Appl. Phys.* 84, 1859 (1998).
18. M. Pavlović and U.V. Desnica, *Jpn. J. Appl. Phys.* 37, 4687 (1998).
19. M. Pavlović, U.V. Desnica, and J. Gladić, *J. Appl. Phys.* 88, 4563 (2000).
20. W.H. Press, B.P. Flannery, S.A. Teukolsky, and W.T. Vetterling, *Numerical Recipes* (Cambridge, U.K.: Cambridge University Press, 1990).
21. P. Silverberg, P. Omling, and L. Samuelson, *Appl. Phys. Lett.* 52, 1689 (1988).
22. D.C. Look, *Semiconductors and Semimetals*, Vol. 19 (New York: Academic Press, 1983).
23. B. Šantić, U.V. Desnica, N. Radić, D.I. Desnica, and M. Pavlović, *J. Appl. Phys.* 73, 5181 (1993).
24. B. Šantić, D.I. Desnica, B.G. Petrović, and U.V. Desnica, *Solid State Commun.* 74, 847 (1990).
25. U.V. Desnica, D.I. Desnica, and B. Šantić, *Appl. Phys. A* 51, 379 (1990).
26. N. Radić and B. Šantić, *Phys. Rev. B* 51, 11117 (1995) and references therein.
27. N. Radić and B. Šantić, *Jpn. J. Appl. Phys.* 34, 75 (1995).

Table III. The Saturation Concentration of the Free Electrons (Holes), $n(\infty)$, ($p(\infty)$), and the Constant K Obtained from the Best Fits for the Respective Photon Energies

E_{ph}/eV	0.7	1.21	1.38
$n(\infty)/\text{cm}^{-3}$	1.2×10^3	3.2×10^8	4.0×10^8
$p(\infty)/\text{cm}^{-3}$	1.4×10^5	5.2×10^6	4.6×10^7
$K = I_{PC}/(10n + p)$	1.8×10^{-16}	0.9×10^{-16}	1.0×10^{-16}
$K = (1.2 \pm 0.5) \times 10^{-16} \text{ A cm}^3$			

28. G.M. Martin, *Appl. Phys. Lett.* 39, 747 (1981).
29. U.V. Desnica, B.G. Petrović, M. Skowronski, and M.C. Cretella, *J. Phys. III France* 1, 1481 (1991).
30. Z.C. Huang, K. Xie, and C.R. Wie, *Rev. Sci. Instrum.* 62, 951 (1991).
31. D.I. Desnica, B. Šantić, and U.V. Desnica, *Appl. Surf. Sci.* 50, 269 (1991).
32. M. Pavlović, U.V. Desnica, N. Radić, and B. Šantić, *Strojarstvo* 38, 287 (1996).
33. A. Mitonneau, A. Mircea, G.M. Martin, and D. Pons, *Rev. Phys. Appl.* 14, 853 (1979).
34. D.C. Look and Z.-Q. Fang, *J. Appl. Phys.* 80, 3590 (1996).
35. D.C. Look, *Electrical Characterization of GaAs Materials and Devices* (New York: Wiley, 1989), p. 95.



DRAFT

Annotations from 889R4.pdf

Page 1

Annotation 1; Label: IPC; Date: 9/4/2003 2:36:57 PM

Is the insertion of "and" okay?

Page 4

Annotation 1; Label: IPC; Date: 9/4/2003 2:37:28 PM

Should all of the terms on the right-hand side be set under the square root?

Page 6

Annotation 1; Label: IPC; Date: 9/4/2003 2:37:58 PM

Table III: Are column heads necessary?

Annotation 2; Label: IPC; Date: 9/4/2003 2:38:17 PM

Reference 20: Opening and closing page numbers?

Annotation 3; Label: IPC; Date: 9/4/2003 2:38:22 PM

Reference 22: Opening and closing page numbers?

Page 7

Annotation 1; Label: IPC; Date: 9/4/2003 2:38:37 PM

Reference 35: Closing page number?

Online Proofing Guidance Page

FIRST STEP:

Install Adobe Acrobat Reader if you do not already have this or another Acrobat product installed on your computer. You can do this free of charge by connecting to the Adobe site and following the instructions at:

<http://www.adobe.com/products/acrobat/readermain.html>

SECOND STEP:

Please download and print your PDF file — we recommend that you save this file to disk, rather than opening it from within your Browser.

From a PC:

1. Right-click on the file/article link.
2. Select “Save Target as”
3. Select a desired location on your computer to save the file to, and click on “Save”
4. Open your PDF file directly with Acrobat Reader or another Acrobat product.
5. Print this file as you normally would with any typical application. Example: Go up to your toolbar, select “File”, select “Print”.

From a MAC:

1. Hold the mouse button down over the link.
 - a. In Internet Explorer, select “Download Link to Disk” from the resulting pop-up menu
 - b. In Netscape, select “Save this Link as” from the resulting pop-up menu
2. Select a desired location on your computer and click on “Save”
3. Open your PDF file directly with Acrobat Reader or another Acrobat product.
4. Print this file as you normally would with any typical application. Example: Go up to your menu bar, select “File”, select “Print”.

THIRD STEP:

Please go through the file you have just printed and thoroughly and clearly mark any revisions you would like to see implemented in your paper. If you have had any changes in phone/fax or e-mail addresses since your paper was submitted, please send us this new information.

FOURTH STEP:

Your revised paper needs to be faxed or mailed to:

IPC Print Services
Attn: Sheryl Dickenson
501 Colonial Drive
St. Joseph, MI 49085
Fax number: 1-269-983-4064

If you have questions regarding your paper in general, you may email or telephone:

IPC Print Services
Attn: Sheryl Dickenson
Email: sdickens@ipcjci.com
Phone: 1-269-983-7412, ext. 529